axioms

IMPACT FACTOR 1.9

Article

Interaction of a Four-Level Atom with a Deformed Quantum Field: Mathematical Model and Quantum Resources

Mariam Algarni, Sayed Abdel-Khalek and Kamal Berrada

Special Issue
Advancements in Applied Mathematics and Computational Physics

Edited by
Dr. Branislav Randjelovic and Prof. Dr. Branislav Vlahovic

MDPI

https://doi.org/10.3390/axioms14030211

axioms

MDPI

Article

Interaction of a Four-Level Atom with a Deformed Quantum Field: Mathematical Model and Quantum Resources

Mariam Algarni [1], Sayed Abdel-Khalek [2] and Kamal Berrada [3,*]

[1] Department of Mathematical Sciences, College of Science, Princess Nourah bint Abdulrahman University, P.O. Box 84428, Riyadh 11671, Saudi Arabia; mmalgarni@pnu.edu.sa
[2] Department of Mathematics and Statistics, College of Science, Taif University, P.O. Box 11099, Taif 21944, Saudi Arabia; sayedquantum@yahoo.co.uk
[3] Department of Physics, College of Science, Imam Mohammad Ibn Saud Islamic University (IMSIU), P.O. Box 90950, Riyadh 11432, Saudi Arabia
* Correspondence: berradakamal@ymail.com

Abstract: We introduce a framework presenting the interaction between a four-level atom (F-LA) and a field mode that begins in a coherent state within the para-Bose field (P-BF). The F-LA is considered in a cascade configuration and initially prepared in the upper level. We display the system dynamics by solving the motion equation. We discuss various dynamical behaviors of fundamental quantum resources used in quantum optics and information tasks, including atomic population inversion, quantum entanglement (QE), and the statistical properties of the P-BF based on the parameters of the quantum model. In this context, we demonstrate the impact of various system parameters on these quantum resources. Finally, we illustrate the dynamic relationships among the quantum resources within the model.

Keywords: para-Bose field; four-level atom; quantum entanglement; statistical properties

MSC: 20-xx; 81-xx

Academic Editors: Branislav Randjelovic and Branislav Vlahovic

Received: 14 November 2024
Revised: 16 February 2025
Accepted: 25 February 2025
Published: 13 March 2025

Citation: Algarni, M.; Abdel-Khalek, S.; Berrada, K. Interaction of a Four-Level Atom with a Deformed Quantum Field: Mathematical Model and Quantum Resources. *Axioms* **2025**, *14*, 211. https://doi.org/10.3390/axioms14030211

1. Introduction

In recent decades, numerous studies have explored extensions and modifications of the bosonic Fock–Heisenberg algebra to enhance various aspects of quantum field theory. Researchers have introduced different q-deformations of the simple harmonic oscillator using Jackson's q-calculus [1–4], leading to novel states associated with q-deformed Lie algebras, including q-coherent states, q-cat states, and q-squeezed states [4–12]. Another significant adaptation is the Wigner algebra, which integrates the reflection operator and the Wigner parameter into its structure. This formulation emerges within bosonic relationships and dynamics, yielding infinite-dimensional para-boson representations as well as finite-dimensional representations linked to parafermions [13]. These generalizations naturally lead to concepts involving para fields and para statistics [14,15].

The Jaynes–Cummings model (JCM) is widely utilized in quantum optics to depict the coupling between a two-level quantum system, such as an atom, and a single quantized mode of an electromagnetic field, adhering to the conditions of the rotating wave approximation [16]. This model has been expanded to encompass multi-photon transitions and various forms of fields, alongside an intensity-dependent coupling between the atom and the quantum field [17,18]. Extensions of the standard JCM have also explored additional levels, including three-level atomic systems [19–23]. In this context, many studies have examined the effects of the Kerr medium [24] and intensity-dependent coupling on the

dynamics of three-level atomic systems. Furthermore, the interaction of two three-level atomic systems with a single-mode field, incorporating multi-photon transitions, has been examined in the presence of a Kerr nonlinear medium and detuning effects [25]. Recently, there has been growing interest in the quantum interaction between four-level atoms and cavity fields, with various configurations being explored [26,27].

Quantum entanglement is a fundamental feature of quantum theory, representing nonlocal correlations among composite quantum systems, where classical descriptions of correlations between subsystems are inadequate. It has been extensively studied in quantum information science [28–32] and is crucial for various applications, including quantum communication, teleportation, quantum entanglement swapping, cryptography, quantum computing, and dense coding [33–39]. The amount of entanglement can be quantified using measures such as von Neumann entropy, concurrence, linear entropy, and entanglement of formation [40,41]. Several methods have been proposed to quantify and identify quantum coherence within quantum systems [42]. Numerous studies have been undertaken to characterize and analyze quantum coherence, gaining significant attention through development and application of coherence quantification measures [43–45].

Beyond the specific domain of quantum optics, the mathematical methodologies and physical principles examined in this study have broader implications across multiple fields of physics. The deformed quantum algebras explored here, particularly para-Bose structures, have been extensively utilized in quantum gravity, where they play a crucial role in models of noncommutative space-time and extensions of the Heisenberg algebra [46–49]. Likewise, in condensed matter physics, these algebraic deformations have been instrumental in characterizing unconventional quantum phases, including topological insulators, superconductors, and quantum Hall systems, wherein fractional statistics arise as a consequence of strong electron correlations [50–53]. Specifically, para-statistics and deformed oscillator algebras provide a robust theoretical framework for investigating anionic excitations, which are fundamental to the description of fractional quantum Hall states and spin-liquid phases [54–56]. Furthermore, these mathematical structures contribute significantly to the theoretical modeling of correlated electron systems and quantum materials exhibiting nontrivial topological properties, where symmetry-protected quantum orders emerge [57–59]. In addition, the quantum resources analyzed in this work, such as entanglement and coherence, hold central importance in quantum information science, quantum computing, and quantum metrology. These properties are essential for advancing quantum cryptographic protocols, enhancing precision measurement techniques, and enabling the development of scalable quantum architectures [38,60–63]. By highlighting these interrelations, this study establishes a framework that extends beyond quantum optics and contributes to the broader landscape of modern physics. Moreover, our approach is closely aligned with recent experimental advances in superconducting qubit systems, engineered quantum states, and cavity quantum electrodynamics, further demonstrating the practical relevance of our findings beyond purely theoretical considerations [64–66].

Our manuscript focuses on examining the degree of entanglement, atomic coherence, and atomic inversion in a bipartite system where a four-level atom is coupled with a para-Bose field. We investigate how field deformation and photon transitions impact the dynamic behavior of quantifiers, particularly when the quantum field originates from a coherent state of the P-BF. The time evolution of entanglement between the four-level atom and para-Bose field is analyzed using quantum entropy, while atomic coherence is evaluated through the l_1 norm.

The manuscript is organized as follows: Section 2 describes the quantum model and dynamics, Section 3 presents the quantum quantifiers and discusses the numerical results, and Section 4 provides our conclusions.

2. Mathematical Model and Dynamics

This section describing the Hamiltonian of the interaction between one-mode P-BF with an F-LA has a state $|k\rangle$ ordered from upper to lower as $|1\rangle - |4\rangle$

$$\widehat{H}_{\text{int}} = \sum_{k=1}^{4} \varpi \left(\hat{a}^{J} |k\rangle \left\langle \mathrm{k}+1 \right| + \hat{\mathrm{a}}^{\dagger \mathrm{J}} \left| \mathrm{k}+1 \right\rangle \langle \mathrm{k}| \right), \tag{1}$$

where ϖ represents the coupling constant between the F-LA and PB-field, J denotes the number of photons exchanged in transitions between (F-LA) and (P-BF), and $\hat{a}^{\dagger}(\hat{a})$ is the creation (annihilation) operator of the quantized field, respectively, acting on the Fock states as

$$\hat{a}^{\dagger}|n\rangle = \sqrt{G(n+1)}|n+1\rangle, \;\; \hat{a}|n\rangle = \sqrt{G(n)}|n-1\rangle. \tag{2}$$

Here, the G is a positive function and is equal to $G(n) = n - \left(\left[\frac{n}{2} \right] - \left[\frac{n+1}{2} \right] \right) q$, and q is the P-BF deformed parameter.

The para-Bose field (P-BF) holds significance as it extends traditional bosonic field theory by introducing parastatistics, modifying the conventional commutation relations of annihilation and creation operators. These operators adhere to a parity-deformed oscillator algebra, where $\{R, \hat{a}\} = \{R, \hat{a}^{\dagger}\} = 0$ and $[\hat{a}, \hat{a}^{\dagger}] = G(N+1) - G(N)$, with $N = \hat{a}^{\dagger}\hat{a} + q(I - R)$, resulting in a more generalized Fock space representation. The operator R, known as the parity operator, is a Hermitian operator satisfying $R^2 = 1$, meaning it has eigenvalues ± 1, which classify states into even and odd parity components. This extension enables the study of systems where particles exhibit characteristics that differ from purely bosonic or fermionic behavior, making it a fundamental concept in quantum optics and quantum field theory [67]. The coherent states in the P-BF are characterized as the eigenstates associated with the field's annihilation operator. These states form an overcomplete and nonorthogonal basis, fulfilling the resolution of identity, akin to Glauber coherent states but with alterations due to parastatistical effects [67]. They exhibit notable quantum properties, such as photon antibunching, where the second-order intensity correlation function demonstrates a decreased probability of detecting two photons simultaneously. Additionally, they follow sub-Poissonian statistics, indicated by a negative Mandel parameter, signifying reduced photon number fluctuations compared to classical light sources [67]. Furthermore, these states show quadrature squeezing, where field quadratures x and p experience noise redistribution, confirming the presence of nonclassical effects [8]. Within the framework of JCM, extended to a single-mode P-BF, these states influence atomic inversion, modify Rabi oscillations, and enhance entanglement.

The final state of the (F-LA)–(P-BF) system at any time $\tau > 0$, where $\tau = \varpi t$ represents the scaled time, can be expressed as:

$$|\psi(\tau)\rangle = \sum_{n=0}^{\infty} \sum_{k=1}^{4} R_j(n, \tau)|n + k - 1, k\rangle. \tag{3}$$

The amplitude $R_j(n, \tau), j = 1, 2, 3, 4$ can be obtained by solving the equation of motion of this system:

$$-i\,\hbar \frac{\partial}{\partial t}|\psi(\tau)\rangle = \widehat{H}_{int}|\psi(\tau)\rangle. \tag{4}$$

At $\tau = 0$, the F-LA in the upper state and the field in the coherent state of the P-BF $|Z, q\rangle$. So, the initial state is assumed to be

$$|\psi(0)\rangle = |\psi_{\text{F-LA}}(0)\rangle \otimes |\psi_{\text{B-PF}}(0)\rangle = |1\rangle \otimes |Z, q\rangle, \tag{5}$$

where $|Z,q\rangle$ are provided as [41]

$$|Z,q\rangle = \frac{\exp\left(-\frac{|Z|^2}{2}\right)4^q\sqrt{(q!)^3}}{\sqrt{(2q)!}}\sum_{n=0}^{\infty} Z^n \sqrt{\frac{(q+\left[\frac{n}{2}\right])!}{\left[\frac{n}{2}\right]!(2q+n)!}} L_q^{[\frac{n-1}{2}]+\frac{1}{2}}\left(\frac{|Z|^2}{2}\right)|n\rangle. \tag{6}$$

Here, Z is the amplitude of the coherent state of the P-BF and $L_q^m(\ldots)$ are the associated Laguerre polynomials.

The coefficients R_j, representing the probability amplitudes, are determined by solving the time-dependent Schrödinger Equation (4) with the initial condition $|\psi(0)\rangle = |Z,q,1\rangle$. Consequently, these coefficients fulfill the following set of coupled differential equations:

$$\frac{d}{dt}\begin{pmatrix} R_1 \\ R_2 \\ R_3 \\ R_4 \end{pmatrix} = \begin{pmatrix} 0 & -i\varpi\sqrt{\frac{(n+J)!}{n!}} & 0 & 0 \\ -i\varpi\sqrt{\frac{(n+J)!}{n!}} & 0 & -i\varpi\sqrt{\frac{(n+2J)!}{(n+J)!}} & 0 \\ 0 & -i\varpi\sqrt{\frac{(n+2J)!}{(n+J)!}} & 0 & -i\varpi\sqrt{\frac{(n+3J)!}{(n+2J)!}} \\ 0 & 0 & -i\varpi\sqrt{\frac{(n+3J)!}{(n+2J)!}} & 0 \end{pmatrix}\begin{pmatrix} R_1 \\ R_2 \\ R_3 \\ R_4 \end{pmatrix}. \tag{7}$$

In this paper, we focus on the effects of single- and double-photon transitions, corresponding to $J = 1$ and 2, respectively. We analyze the time-dependent features of various quantum quantifiers related to the quantum system under investigation using the wave function $|\psi(\tau)\rangle$ (see Appendix A).

The atomic population inversion, quantum entropy, and coherence are all linked to the components of the atomic density matrix $\rho^{\text{F-LA}}(\tau)$, which is given by

$$\rho^{F\text{-}LA}(\tau) = Tr_{P\text{-}BF}|\psi(\tau)\rangle\left\langle\psi(\tau)\right| = \sum_{r=1}^{4}\sum_{l=1}^{4}\rho_{rl}(\tau)\left|r\right\rangle\langle l|. \tag{8}$$

The P-BF density matrix can be obtained as $\rho_{P\text{-BF}}(\tau) = Tr_{\text{F-LA}}|\psi(\tau)\rangle\langle\psi(\tau)| = \sum_m^{\infty}\rho_m|m\rangle\langle m|$.

3. Quantum Quantifiers

To investigate the effect of the P-BF deformed parameter q and single- and double-photon transition on the dynamics of quantum quantifiers, in Figures 1–4 illustrate the time-dependent behavior of the atomic inversion, second-order correlation function (S-OCF), atomic entropy, and atomic coherence.

3.1. Population Inversion Corresponding to the F-LA

Population inversion is one of the most significant quantities when considering quantum information. It can be applied to determine the collapse and revival times, which are crucial for characterizing the maximally entangled and separable state periods. We define the atomic population inversion through the diagonal elements of the atomic density matrix $\rho^{\text{F-LA}}(\tau)$ as

$$\rho_Z(\tau) = \rho_{11}(\tau) - \rho_{44}(\tau). \tag{9}$$

3.2. Nonclassical Effects

The S-OCF is widely employed to investigate the statistical characteristics of the field, as well as to assess photon bunching or antibunching phenomena. It is defined as:

$$g^{(2)}(\tau) = \frac{\left\langle\widehat{L}^{\dagger 2}\widehat{L}^2\right\rangle}{\left\langle\widehat{L}^{\dagger}\widehat{L}\right\rangle^2}. \tag{10}$$

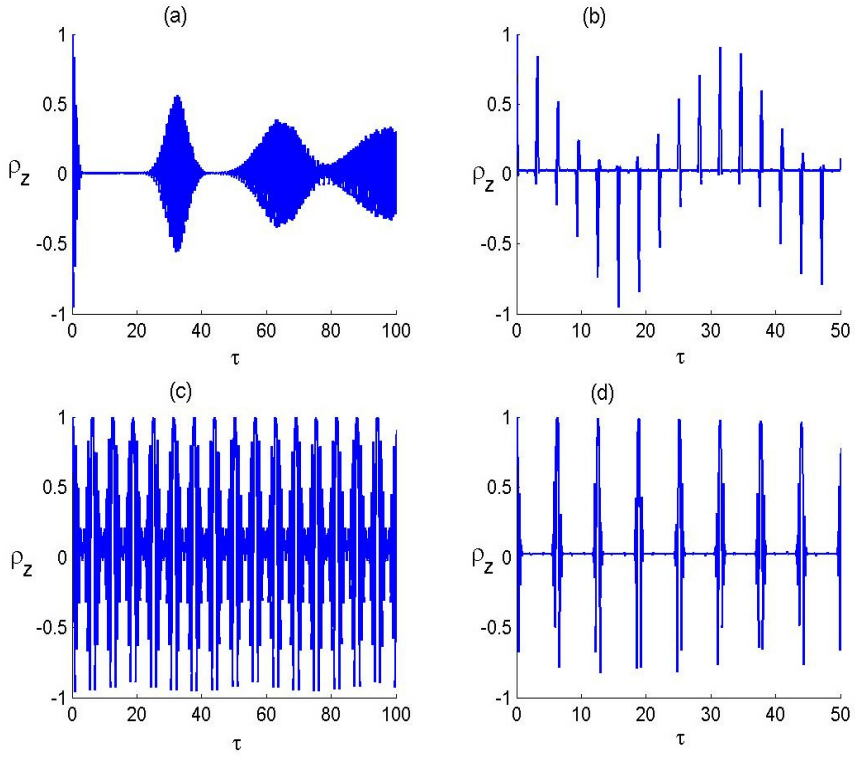

Figure 1. Dynamics of the atomic inversion ρ_Z of F-LA with $z = 4$ and for the parameter values of P-BF deformed parameter q and number of photons transitioned J as (**a**) $(q, J) = (0, 1)$, (**b**) $(q, J) = (0, 2)$, (**c**) $(q, J) = (20, 1)$, and (**d**) $(q, J) = (20, 2)$.

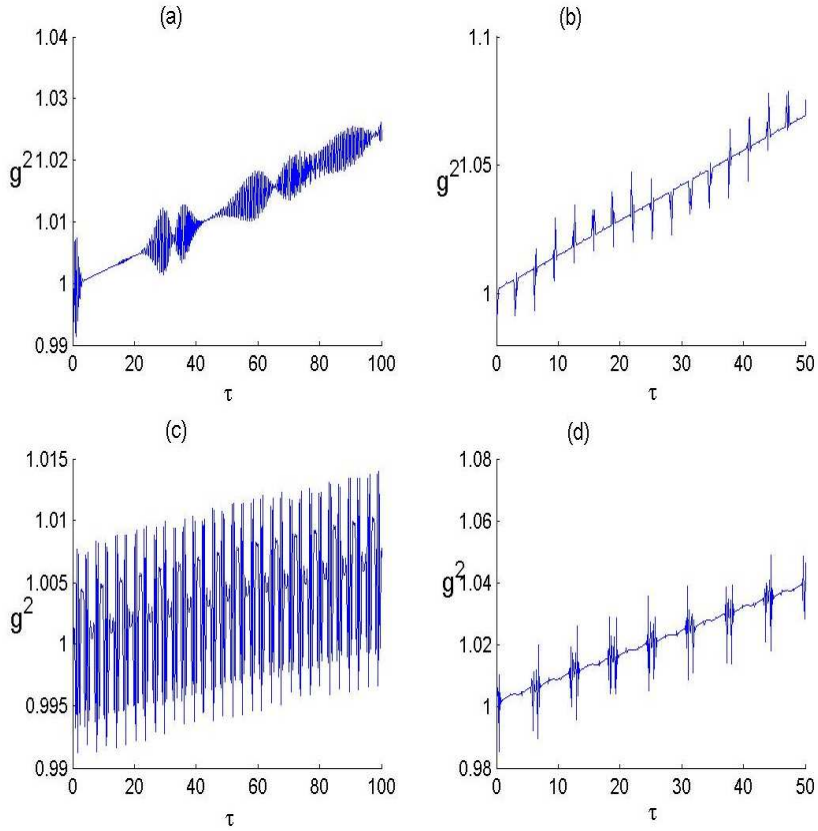

Figure 2. Dynamics of the S-OCF g^2, with $z = 4$ and for the parameter values of P-BF deformed parameter q and number of photons transitioned J as (**a**) $(q, J) = (0, 1)$, (**b**) $(q, J) = (0, 2)$, (**c**) $(q, J) = (20, 1)$, and (**d**) $(q, J) = (20, 2)$.

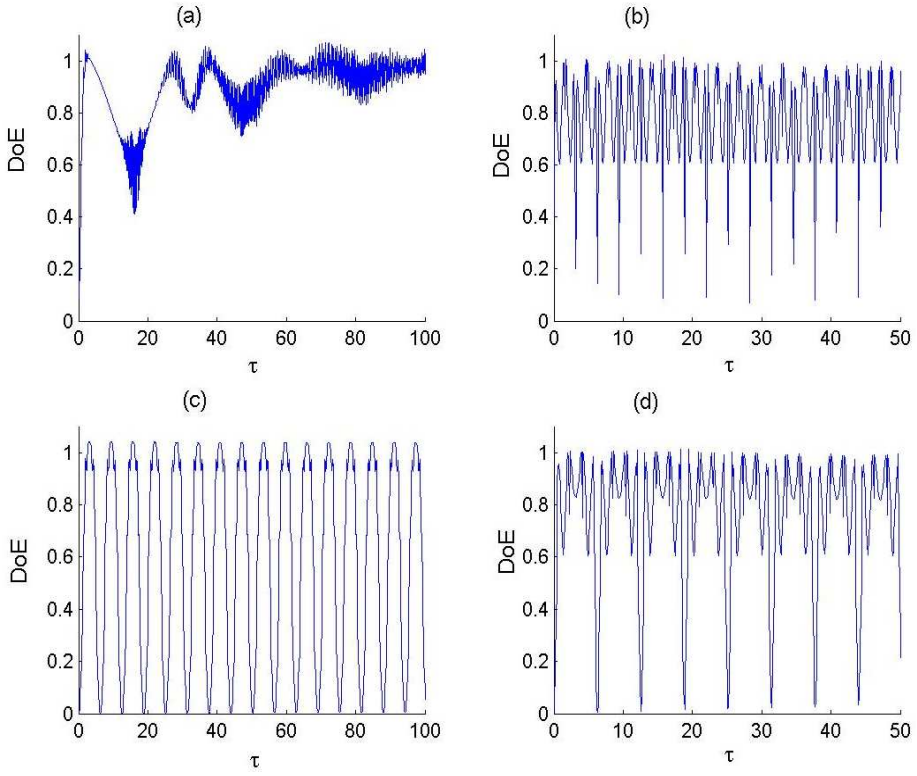

Figure 3. Dynamics of the $S_{F\text{-}LA}$ as a measure of QE between F-LA and P-BF with $z = 4$ and for the parameter values of P-BF deformed parameter q and number of photons transitioned J as (**a**) $(q, J) = (0, 1)$, (**b**) $(q, J) = (0, 2)$, (**c**) $(q, J) = (20, 1)$, and (**d**) $(q, J) = (20, 2)$.

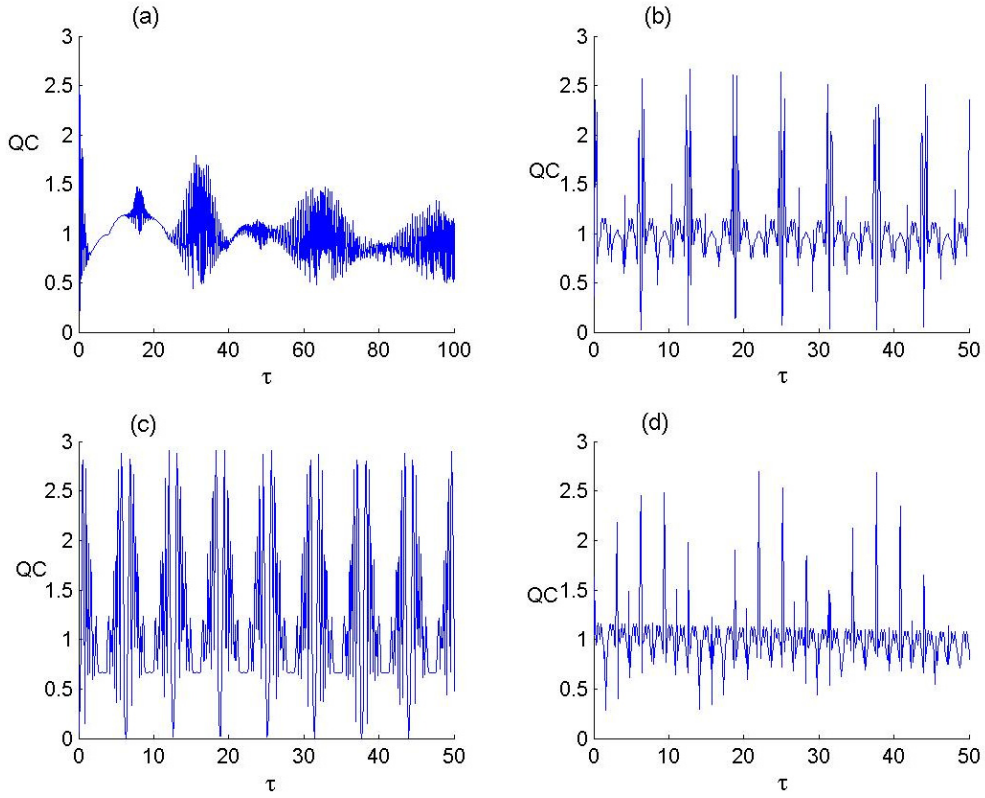

Figure 4. Dynamics of the quantum coherence Q_C, of F-LA with $z = 4$ and for the parameter values of P-BF deformed parameter q and number of photons transitioned J as (**a**) $(q, J) = (0, 1)$, (**b**) $(q, J) = (0, 2)$, (**c**) $(q, J) = (20, 1)$, and (**d**) $(q, J) = (20, 2)$.

We say that the quantized field is governed by super-Poissonian statistics if $g^{(2)} > 1$, Poissonian statistics if $g^{(2)} = 1$, and sub-Poissonian statistics if $g^{(2)} < 1$. The sub-Poissonian distribution of photons illustrates the quantum nature of the field.

3.3. Quantum Entanglement

The subsystem entropy, defined by the von Neumann entropy, can be used to determine the degree of entanglement (DoE) evolution of the (F-LA)–(P-BF) state. It is given by

$$DoE = -\mathrm{Tr}\left\{\rho^{\text{F-LA}}(\tau)\ln\left[\rho^{\text{F-LA}}(\tau)\right]\right\}, \tag{11}$$

where $\rho^{\text{F-LA}}(\tau)$ represents the F-LA density operator, as given by Equation (8). Based on refs. [40,41], the function $DoE_{(\text{F-LA})-(\text{P-BF})}$ takes the following form:

$$DoE_{(F\text{-}LA)-(P\text{-}BF)} = -\sum_{j=1}^{4} r_j ln r_j, \tag{12}$$

where r_j is the jth eigenvalue of the state $\rho^{\text{F-LA}}$.

3.4. Quantum Coherence

The diagonal components of the system's density operator delineate the essential properties of coherence. The quantum coherence is determined by considering the absolute value of the non-diagonal elements and applying the l_1 norm. The coherence measure is the distance between the state in question and the nearest incoherent state from the point of view of the concept of entropy. To detect the amount of coherence, we consider the l_1 norm of coherence. This measure depends on off-diagonal elements for the density operator and it is defined by the formula [42]:

$$Q_c = \sum_{\substack{kl \\ k \neq l}} |\rho_{kl}|, \tag{13}$$

4. Numerical Results and Discussion

Figure 1 illustrates the dynamics of atomic population inversion in the F-LA system interacting with the P-BF under conditions of zero and non-zero deformation parameters, considering both single- and double-photon transitions. For a zero-deformation parameter, panels (a) and (b) depict the time evolution of atomic population for single- and double-photon excitations, respectively. In the single-photon excitation case, we observe distinct features of collapses and revivals in atomic population inversion. Initially, the collapses are well defined within the scaled time, but they become less distinct over time, with the revival amplitude gradually diminishing. In the double-photon excitation scenario, the atomic population exhibits brief revivals interspersed with adjacent collapses. These revivals are asymmetric around the zero-population inversion line, with fluctuations between positive and negative values of +1 and -1. The revival duration is notably shorter compared to the single-photon case. Panels (c) and (d) present the dynamics for a non-zero deformation parameter, set at 20 scaled units, for single- and double-photon transitions. In the single-photon case, we observe revivals in atomic population with very brief collapses, and the revival amplitude spans the entire range of population values. For the double-photon transition with a non-zero deformation parameter, the dynamics show collapses and revivals similar to the single-photon case, but with an increased collapse duration and a slightly reduced oscillation amplitude. Comparing the effects of varying photon transition numbers and deformation parameters, it is evident that these factors significantly influence the population inversion dynamics. For $q = 20$, increasing J from 1 to 2 leads to more frequent revivals and a reduction in their width. Conversely, for $q = 20$, increasing J

does not increase the number of revivals but shortens the revival span. The collapse and revival phenomena observed in atom-field interactions indicate coherent quantum evolution, where revivals stem from constructive interference among atomic state amplitudes, while collapse periods reflect decoherence effects caused by transitions between energy levels. These results are consistent with previous research on Jaynes–Cummings models and intensity-dependent atom-field interactions, where nonlinearity and deformation significantly influence atomic transition dynamics. In particular, studies on q-deformed oscillators and para-Bose models reveal that deformation alters energy spectra and transition rates, leading to extended coherence times and modified revival patterns. The alignment of these findings with theoretical predictions in nonlinear optics and quantum field theories suggests that para-Bose field deformation serves as a controllable parameter for regulating atomic inversion dynamics.

Figure 2 shows the evolution of S-OCF g^2 for the F-LA system under conditions of zero and non-zero deformation parameters q, considering both single- and double-photon transitions $J = 1, 2$, respectively. For $q = 0$, we can observe that $g^{(2)} < 1$ at the beginning of interaction for $J = 1, 2$, indicating sub-Poissonian statistics. As the time increases, the function $g^{(2)}$ becomes larger than 1, indicating super-Poissonian statistics. For $q = 20$, we can observe that the function $g^{(2)}$ exhibits an oscillatory behavior with values greater and smaller than one, indicating super- and sub-Poissonian statistics. In the case of $J = 2$, we have $g^{(2)} < 1$ at the beginning of interaction and $g^{(2)} > 1$ as the time increases. The shift from sub- to super-Poissonian statistics suggests that interaction time significantly influences photon distribution. Studies on q-deformed oscillators and para-Bose fields demonstrate that deformation alters photon statistics by introducing nonlinear effects, leading to oscillatory behavior in $g^{(2)}$ for $q = 20$. Similar patterns have been observed in nonlinear quantum optics, such as Kerr media, where nonlinearity modulates photon distribution, indicating that para-Bose deformation introduces an additional degree of complexity to photon dynamics. The tunability of photon statistics enables the design of nonclassical light sources. Para-Bose deformation provides a useful method for controlling photon statistics, contributing to advancements in quantum optics applications.

Figure 3 displays the quantum entanglement (QE), as measured by the von Neumann entropy, for the F-LA–P-BF state under varying field deformation and photon transition numbers. For q = 0, panels (a) and (b) depict the $S_{F\text{-}LA}$ dynamics for single-photon (J = 1) and double-photon (J = 2) transitions, respectively. In the single-photon case, rapid oscillations are observed in the entanglement measure, with the amplitude fluctuating around a steady-state value before eventually stabilizing. In contrast, for the double-photon transition (J = 2), the entanglement exhibits quasi-periodic behavior. Unlike the single-photon case, the entanglement measure does not settle into a steady state. Panels (c) and (d) show the time-dependent behavior of entanglement for a non-zero field deformation parameter q for both single- and double-photon transitions, respectively. For J = 1, the function $S_{F\text{-}LA}$ exhibits consistent periodic behavior with a constant amplitude of oscillations throughout the dynamics. In the double-photon transition case (J = 2), the QE dynamics also display periodicity, but the amplitude of oscillations varies over time, introducing an additional layer of complexity to the system's behavior. Thus, the consideration of field deformation and double-photon transitions enhances the periodic nature of the entanglement measure during the evolution. These observations align with established studies in quantum optics, particularly the JCM, where single-photon transitions typically lead to periodic entanglement oscillations, while multi-photon transitions introduce interactions that increase quantum correlations. The quasi-periodic behavior in the J = 2 case suggests an enhanced interaction mechanism, as multi-photon absorption–emission processes can induce more complex quantum correlations. Studies on q-deformed oscillators and para-Bose fields have

shown that deformation modifies energy levels and transition dynamics, which explains the stable periodic behavior in the J = 1 case and the varying oscillation amplitude in the J = 2 case. Additionally, entanglement dynamics in nonlinear quantum optics, such as Kerr-type media, exhibit similar periodic structures, indicating that para-Bose deformation effectively introduces an adjustable nonlinearity that influences quantum correlations. The ability to control entanglement oscillations through deformation and photon transition tuning presents promising applications in different tasks in quantum information and optics.

Figure 4 displays the dynamics of QC for the F-LA system for both zero and non-zero deformation parameters q of the P-BF, considering single- and double-photon transitions. For the zero-deformation parameter case, the dynamics of QC for single- and double-photon transitions are shown in panels (a) and (b), respectively. In the single-photon case, the QC dynamics exhibit collapses and revivals, with the collapse line fluctuating around a value of 1. In contrast, for the double-photon transition (J = 2), periodic behavior is observed in the QC dynamics, characterized by increased amplitude fluctuations and a shorter revival width compared to the single-photon case. Notably, no collapses are present in this scenario. For the non-zero deformation parameter case, the QC dynamics for single-photon transitions show periodic behavior with an increased amplitude of oscillations compared to the zero-deformation case. In the double-photon transition case (J = 2), oscillations are observed in the QC dynamics, but the amplitude of these oscillations varies over time, indicating more complex dynamic behavior. In summary, the introduction of non-zero deformation parameters enhances the periodic nature of quantum coherence, with single-photon transitions leading to more pronounced oscillations, while double-photon transitions result in oscillations with varying amplitude.

5. Conclusions

In this study, we have explored the dynamics of atomic population inversion, S-OCF, degree of entanglement, and quantum coherence in the F-LA system interacting with the P-BF under both zero and non-zero deformation parameters. For zero deformation parameter values, the system exhibits characteristic collapses and revivals in atomic population inversion during single-photon transitions, while double-photon transitions lead to brief, asymmetric revivals. The S-OCF similarly shows collapses and revivals, with an increasing slope of the collapse line that remains constant across both single- and double-photon transitions. The entanglement dynamics under single-photon transitions oscillate rapidly, stabilizing around a steady state, whereas double-photon transitions induce periodicity without reaching a steady state. Quantum coherence dynamics for single-photon excitations display collapses and revivals, with a collapse line that fluctuates around a steady value. The introduction of non-zero deformation parameters adds additional complexity to the system. For atomic population inversion, the period of oscillation remains the same as in the single-photon transition case, but with an extended collapse duration. The S-OCF and quantum coherence exhibit periodic behaviors, with increased amplitude and variable oscillations, particularly in double-photon transitions. The entanglement dynamics also show enhanced periodicity under non-zero deformation, highlighting the effects of deformation parameter and photon transition numbers on the overall system behavior. Overall, this work highlights the significant impact of field deformation and photon transition numbers on the quantum dynamics of the F-LA system. It provides valuable insights into how these parameters can be effectively controlled to extract and optimize quantum resources from the system. Regarding the experimental feasibility of our findings, we highlight that our model, which considers the interaction between a four-level atom and a deformed para-Bose field, can be realized using trapped atoms or ions in cavity quantum electrodynamics setups, where four-level atomic structures naturally arise in alkali or alkaline-earth

atoms through well-defined energy level configurations. Another promising platform is cold atoms in optical lattices, where multi-level atomic transitions can be engineered via laser coupling.

Author Contributions: M.A.: investigation (equal); methodology (equal); software (equal); writing—original draft (equal). S.A.-K.: investigation (equal); methodology (equal); writing—review and editing (equal). K.B.: investigation (equal); resources (equal); writing—original draft (equal). All authors have read and agreed to the published version of the manuscript.

Funding: Princess Nourah bint Abdulrahman University Researchers Supporting Project number (PNURSP2025R225), Princess Nourah bint Abdulrahman University, Riyadh, Saudi Arabia.

Data Availability Statement: Not applicable.

Acknowledgments: The authors acknowledge to Princess Nourah bint Abdulrahman University Researchers Supporting Project number (PNURSP2025R225), Princess Nourah bint Abdulrahman University, Riyadh, Saudi Arabia.

Conflicts of Interest: The authors declare no conflict of interest.

Appendix A. Detailed Calculation

The evolution of the quantum state of the system is governed by the time-dependent Schrödinger equation:

$$i\hbar\frac{\partial}{\partial t}|\psi(t)\rangle = \widehat{H}_{\text{int}}|\psi(t)\rangle, \tag{A1}$$

where $\widehat{H}_{\text{int}}$ represents the interaction Hamiltonian describing the coupling between the four-level atom and the para-Bose field. The objective is to express this equation in terms of a set of differential equations governing the probability amplitudes associated with the atomic and field states.

Given that the system comprises an atom possessing four distinct energy levels coupled to a quantized field mode, the wavefunction is articulated as a superposition of the atomic states and the field's Fock states:

$$|\psi(t)\rangle = \sum_{k=1}^{4}\sum_{n=0}^{\infty} R_k(n,t)|n+k-1,k\rangle, \tag{A2}$$

where $R_k(n,t)$ represents the probability amplitude for the atom being in state $|k\rangle$ with $n+k-1$ photons in the field. Substituting this expansion into the Schrödinger equation and differentiating,

$$i\hbar\sum_{k=1}^{4}\sum_{n=0}^{\infty}\frac{dR_k(n,t)}{dt}|n+k-1,k\rangle = \widehat{H}_{\text{int}}\sum_{k=1}^{4}\sum_{n=0}^{\infty} R_k(n,t)|n+k-1,k\rangle. \tag{A3}$$

Multiplying both sides by $\langle n+k-1,k|$ and utilizing the orthonormality of the basis states, we obtain

$$i\hbar\frac{dR_k(n,t)}{dt} = \sum_{j=1}^{4}\langle n+k-1,k|\widehat{H}_{\text{int}}|n+j-1,j\rangle R_j(n,t). \tag{A4}$$

This equation provides a framework for obtaining the system of differential equations once we determine the Hamiltonian matrix elements. The interaction Hamiltonian for the quantum system is expressed as:

$$\widehat{H}_{\text{int}} = \sum_{k=1}^{4}\varpi\left(\hat{L}^{J}|k\rangle\left\langle \mathrm{k}+1\right|+\hat{\mathrm{L}}^{\dagger \mathrm{J}}\left|\mathrm{k}+1\right\rangle\langle \mathrm{k}|\right), \tag{A5}$$

The operators and $\hat{L}^{\dagger}$ and $\hat{L}$ govern the transitions between atomic levels, leading to the coupling terms in the equations of motion. Using the matrix elements obtained from the

Hamiltonian action on the basis states, we obtain at the final system of coupled differential equations. The probability amplitudes evolve according to:

$$\frac{d}{dt}\begin{bmatrix} R_1 \\ R_2 \\ R_3 \\ R_4 \end{bmatrix} = \begin{bmatrix} 0 & -i\omega\sqrt{\frac{(n+J)!}{n!}} & 0 & 0 \\ -i\omega\sqrt{\frac{(n+J)!}{n!}} & 0 & -i\omega\sqrt{\frac{(n+2J)!}{(n+J)!}} & 0 \\ 0 & -i\omega\sqrt{\frac{(n+2J)!}{(n+J)!}} & 0 & -i\omega\sqrt{\frac{(n+3J)!}{(n+2J)!}} \\ 0 & 0 & -i\omega\sqrt{\frac{(n+3J)!}{(n+2J)!}} & 0 \end{bmatrix} \begin{bmatrix} R_1 \\ R_2 \\ R_3 \\ R_4 \end{bmatrix}. \tag{A6}$$

This system provides a full description of the time evolution of the probability amplitudes, incorporating the effects of multi-photon transitions and field deformation.

To determine the probability amplitudes $R_k(n,t)$, we solve the system of coupled differential equations. This system can be expressed in matrix form as

$$\frac{d}{dt}\mathrm{R}(t) = \mathrm{M}\mathrm{R}(t), \tag{A7}$$

where $\mathrm{R}(t)$ is the column vector of probability amplitudes and M is the coupling matrix. Since the matrix M is time-independent, the formal solution can be obtained using matrix exponentiation:

$$\mathrm{R}(t) = e^{\mathrm{M}t}\mathrm{R}(0). \tag{A8}$$

If M is diagonalizable, we write it as $\mathrm{M} = \mathrm{V}\mathrm{D}\mathrm{V}^{-1}$, leading to the solution:

$$\mathrm{R}(t) = \mathrm{V}e^{\mathrm{D}t}\mathrm{V}^{-1}\mathrm{R}(0), \tag{A9}$$

where V is the matrix whose columns are the eigenvectors of M, and $e^{\mathrm{D}t}$ is a diagonal matrix with elements $e^{\lambda_i t}$, where λ_i are the eigenvalues of M. Alternatively, numerical-method techniques can be used. Once the amplitudes $R_k(n,t)$ are determined, they allow analysis of quantum properties such as atomic population inversion, quantum coherence, and entanglement.

References

1. Arik, M.; Coon, D.D. Hilbert spaces of analytic functions and generalized coherent states. *J. Math. Phys.* **1976**, *17*, 524. [CrossRef]
2. Biedenharn, L.C. The quantum group SU_q (2) and a q-analogue of the boson operators. *J. Phys. A Math. Gen.* **1989**, *22*, L873. [CrossRef]
3. Macfarlane, A.J. On q-analogues of the quantum Harmonic oscillator and the quantum group *SU* (2). *J. Phys. A Math. Gen.* **1989**, *22*, 4581. [CrossRef]
4. Fakhri, H.; Nouraddini, M. Right SU_q (2)- and left SU_{q-1} (2)-invariances of the q-Hilbert–Schmidt scalar products for an adjoint representation of the quantum algebra $\breve{U}_q$ (su_2). *J. Geom. Phys.* **2016**, *110*, 90. [CrossRef]
5. Fakhri, H.; Hashemi, A. Nonclassical properties of the q-coherent and q-cat states of the Biedenharn–Macfarlane q oscillator with q > 1. *Phys. Rev. A* **2016**, *93*, 013802. [CrossRef]
6. Fakhri, H.; Sayyah-Fard, M. Arik-Coon q-oscillator cat states on the noncommutative complex plane and their nonclassical properties. *Int. J. Geom. Meth. Mod. Phys.* **2017**, *14*, 1750060. [CrossRef]
7. Fakhri, H.; Sayyah-Fard, M. Nonclassical properties of the Arik-Coon q−1-oscillator coherent states on the noncommutative complex plane Cq. *Int. J. Geom. Meth. Mod. Phys.* **2017**, *14*, 1750165. [CrossRef]
8. Fakhri, H.; Sayyah-Fard, M. q-coherent states associated with the noncommutative complex plane C q^2 for the Biedenharn–Macfarlane q-oscillator. *Ann. Phys.* **2017**, *387*, 14. [CrossRef]
9. Fakhri, H.; Sayyah-Fard, M. Triplet q-cat states of the Biedenharn–Macfarlane q-oscillator with q > 1. *Quantum Inf. Process.* **2020**, *19*, 19. [CrossRef]
10. Fakhri, H.; Mousavi-Gharalari, S.E. Nonclassical properties of two families of q-coherent states in the Fock representation space of q-oscillator algebra. *Eur. Phys. J. Plus* **2020**, *135*, 253. [CrossRef]
11. Fakhri, H.; Sayyah-Fard, M. Noncommutative photon-added squeezed vacuum states. *Mod. Phys. Let. A* **2020**, *35*, 2050167. [CrossRef]

12. Sayyah-Fard, M. Nonclassicality of photon-added q-squeezed first excited states. *Phys. A* **2021**, *567*, 125636. [CrossRef]
13. Plyushchay, M.S. Deformed Heisenberg algebra with reflection. *Nucl. Phys. B* **1997**, *491*, 619. [CrossRef]
14. Wigner, E.P. Do the equations of motion determine the quantum mechanical commutation relations? *Phys. Rev.* **1950**, *77*, 711. [CrossRef]
15. Green, H.S. A generalized method of field quantization. *Phys. Rev.* **1953**, *90*, 270. [CrossRef]
16. Jaynes, E.T.; Cummings, F.W. Comparison of quantum and semiclassical radiation theories with application to the beam maser. *Proc. IEEE* **1963**, *51*, 89–109. [CrossRef]
17. Abdel-Aty, M. General formalism of interaction of a two-level atom with cavity field in arbitrary forms of nonlinearities. *Phys. A* **2002**, *313*, 471. [CrossRef]
18. Baghshahi, H.R.; Tavassoly, M.K. Entanglement, quantum statistics and squeezing of two Ξ-type three-level atoms interacting nonlinearly with a single-mode field. *Phys. Scr.* **2014**, *89*, 075101. [CrossRef]
19. Feneuile, S. Interaction of laser radiation with free atoms. *Rep. Prog. Phys.* **1977**, *40*, 1257. [CrossRef]
20. Li, X.-S.; Lin, D.L.; Gong, C.D. Nonresonant interaction of a three-level atom with cavity fields. I. General formalism and level occupation probabilities. *Phys. Rev. A* **1987**, *36*, 5209. [CrossRef]
21. Liu, Z.-D.; Li, X.-S.; Lin, D.L. Nonresonant interaction of a three-level atom with cavity fields. II. Coherent properties of the stimulated fields. *Phys. Rev. A* **1987**, *36*, 5220. [CrossRef]
22. Abdel-Wahab, N.H. The general formalism for a three-level atom interacting with a two-mode cavity field. *Phys. Scr.* **2007**, *76*, 233. [CrossRef]
23. Abdel-Wahab, N.H. A three-level atom interacting with a single mode cavity field: Different configurations. *Phys. Scr.* **2007**, *76*, 244. [CrossRef]
24. Yurke, B.; Stoler, D. One-step synthesis of multiatom Greenberger-Horne-Zeilinger states. *Phys. Rev. Lett.* **1993**, *57*, 13. [CrossRef] [PubMed]
25. Wang, H.; Goorskey, D.; Xiao, M. Dependence of enhanced Kerr nonlinearity on coupling power in a three-level atomic system. *Opt. Lett.* **2002**, *27*, 258–260. [CrossRef]
26. Baghshahi, H.R.; Tavassoly, M.K. Dynamics of different entanglement measures of two three-level atoms interacting nonlinearly with a single-mode field. *Eur. Phys. J. Plus* **2015**, *130*, 37. [CrossRef]
27. Liu, Z.D.; Zhu, S.-Y.; Li, X.-S. The properties of a light field interacting with a four-level atom. *J. Mod. Opt.* **1988**, *45*, 833. [CrossRef]
28. Vaglica, A.; Vetri, G. Irreversible decay of nonlocal entanglement via a reservoir of a single degree of freedom. *Phys. Rev. A* **2007**, *75*, 062120. [CrossRef]
29. Ficek, Z.; Tanas, R. Dark periods and revivals of entanglement in a two-qubit system. *Phys. Rev. A* **2006**, *74*, 024304. [CrossRef]
30. Vitali, D.; Gigan, S.; Ferreira, A.; Böhm, H.R.; Tombesi, P.; Guerreiro, A.; Vedral, V.; Zeilinger, A.; Aspelmeyer, M. Optomechanical entanglement between a movable mirror and a cavity field. *Phys. Rev. Lett.* **2007**, *98*, 030405. [CrossRef]
31. Zhang, Q.; Zhang, E.Y. Optimum parameters for biased two-state quantum key distribution protocol. *Acta Phys. Sin.* **2002**, *51*, 1684.
32. Moller, C. Dissipative Rabi model in the dispersive regime. *Phys. Rev. Res.* **2020**, *2*, 033046. [CrossRef]
33. Bennett, C.H.; Brassard, G.; Crépeau, C.; Jozsa, R.; Peres, A.; Wootters, W.K. Teleporting an unknown quantum state via dual classical and Einstein-Podolsky-Rosen channels. *Phys. Rev. Lett.* **1993**, *70*, 1895. [CrossRef] [PubMed]
34. Metwally, N.; Abdelaty, M.; Obada, A.-S.F. Quantum teleportation via entangled states generated by the Jaynes–Cummings model. *Chaos Solitons Fractals* **2004**, *22*, 529. [CrossRef]
35. Ekert, A.K. Quantum cryptography based on Bell's theorem. *Phys. Rev. Lett.* **1991**, *67*, 661. [CrossRef]
36. Bennett, C.H.; Wiesner, S.J. Communication via one-and two-particle operators on Einstein-Podolsky-Rosen states. *Phys. Rev. Lett.* **1992**, *69*, 2881. [CrossRef]
37. Yang, M.; Song, W.; Cao, Z.L. Entanglement swapping without joint measurement. *Phys. Rev. A* **2005**, *71*, 034312. [CrossRef]
38. Nielsen, M.A.; Chuang, I.L. *Quantum Computation and Quantum Information*; Cambridge University Press: Cambridge, UK, 2000.
39. Bennett, C.H.; Shor, P.W.; Smolin, J.A.; Thapliyal, A.V. Entanglement-assisted classical capacity of noisy quantum channels. *Phys. Rev. Lett.* **1999**, *83*, 3081. [CrossRef]
40. Phoenix, S.J.D.; Knight, P.L. Establishment of an entangled atom-field state in the Jaynes-Cummings model. *Phys. Rev. A* **1991**, *44*, 6023. [CrossRef]
41. Phoenix, S.J.D.; Knight, P. Comment on "Collapse and revival of the state vector in the Jaynes-Cummings model: An example of state preparation by a quantum apparatus". *Phys. Rev. Lett.* **1991**, *66*, 2833. [CrossRef]
42. Baumgratz, T.; Cramer, M.; Plenio, M.B. Quantifying coherence. *Phys. Rev. Lett.* **2014**, *113*, 140401. [CrossRef]
43. Berrada, K.; Algarni, M.; Marin, M.; Abdel-Khalek, S. Effects of Dipole-Dipole Interaction and Time-Dependent Coupling on the Evolution of Entanglement and Quantum Coherence for Superconducting Qubits in a Nonlinear Field System. *Symmetry* **2023**, *15*, 732. [CrossRef]

44. Algarni, M.; Berrada, K.; Abdel-Khalek, S. Quantum coherence and parameter estimation for mixed entangled coherent states. *Mod. Phys. Lett. A* **2022**, *37*, 2250159. [CrossRef]
45. Abdel-Khalek, S.; Algarni, M.; Marin, M.; Berrada, K. Entanglement, quantum coherence and quantum Fisher information of two qubit-field systems in the framework of photon-excited coherent states. *Opt. Quant. Elect.* **2023**, *55*, 1288. [CrossRef]
46. Majid, S. *Foundations of Quantum Group Theory*; Cambridge University Press: Cambridge, UK, 1995.
47. Madore, J. Noncommutative Geometry for Pedestrians. *Phys. Rep.* **1997**, *282*, 1.
48. Snyder, H.S. Quantized Space-Time. *Phys. Rev.* **1947**, *71*, 38. [CrossRef]
49. Freidel, L.; Livine, E.R. Ponzano-Regge model revisited III: Feynman diagrams and effective field theory. *Class. Quantum Grav.* **2006**, *23*, 2021. [CrossRef]
50. Wen, X.-G. *Quantum Field Theory of Many-Body Systems*; Oxford University Press: Oxford, UK, 2004.
51. Nayak, C.; Simon, S.H.; Stern, A.; Freedman, M.; Das Sarma, S. Non-Abelian anyons and topological quantum computation. *Rev. Mod. Phys.* **2008**, *80*, 1083. [CrossRef]
52. Das Sarma, S.; Freedman, M.; Nayak, C. Topologically protected qubits from a possible non-Abelian fractional quantum Hall state. *Phys. Rev. Lett.* **2005**, *94*, 166802. [CrossRef]
53. Read, N.; Rezayi, E. Beyond paired quantum Hall states: Parafermions and incompressible states in the first excited Landau level. *Phys. Rev. B* **1999**, *59*, 8084. [CrossRef]
54. Moore, G.; Read, N. Nonabelions in the fractional quantum Hall effect. *Nucl. Phys. B* **1991**, *360*, 362. [CrossRef]
55. Kitaev, A. Fault-tolerant quantum computation by anyons. *Ann. Phys.* **2003**, *303*, 2. [CrossRef]
56. Wen, X.-G. Topological orders and edge excitations in fractional quantum Hall states. *Adv. Phys.* **1995**, *44*, 405. [CrossRef]
57. Bernevig, B.A.; Hughes, T.L.; Zhang, S.C. Quantum spin Hall effect and topological phase transition in HgTe quantum wells. *Science* **2006**, *314*, 1757. [CrossRef]
58. Hasan, M.Z.; Kane, C.L. Topological insulators. *Rev. Mod. Phys.* **2010**, *82*, 3045. [CrossRef]
59. Kitaev, A. Periodic table for topological insulators and superconductors. *AIP Conf. Proc.* **2009**, *1134*, 22.
60. Bennett, C.H.; Brassard, G. Quantum cryptography: Public key distribution and coin tossing. *Theor. Comput. Sci.* **2014**, *560 Pt 1*, 7–11. [CrossRef]
61. Braunstein, S.L.; Caves, C.M. Statistical distance and the geometry of quantum states. *Phys. Rev. Lett.* **1994**, *72*, 3439. [CrossRef]
62. Dowling, J.P.; Milburn, G.J. Quantum technology: The second quantum revolution. *Phil. Trans. R. Soc. A* **2003**, *361*, 1655. [CrossRef]
63. Kimble, H.J. The quantum internet. *Nature* **2008**, *453*, 1023. [CrossRef]
64. Clarke, J.; Wilhelm, F.K. Superconducting quantum bits. *Nature* **2008**, *453*, 1031. [CrossRef] [PubMed]
65. Barends, R.; Kelly, J.; Megrant, A.; Veitia, A.; Sank, D.; Jeffrey, E.; White, T.C.; Mutus, J.; Fowler, A.G.; Campbell, B.; et al. Superconducting quantum circuits at the surface code threshold for fault tolerance. *Nature* **2014**, *508*, 500. [CrossRef] [PubMed]
66. Haroche, S.; Raimond, J.-M. *Exploring the Quantum: Atoms, Cavities, and Photons*; Oxford University Press: Oxford, UK, 2006.
67. Fakhri, H.; Sayyah-Fard, M. The Jaynes–Cummings model of a two-level atom in a single-mode para-Bose cavity field. *Sci. Rep.* **2021**, *11*, 22861. [CrossRef] [PubMed]